Mechanistic insight into reactivity of sulfate radical with aromatic contaminants through single-electron transfer pathway

CrossMark

Shuang Luo [a,b,1], Zongsu Wei [c,1], Dionysios D. Dionysiou [d], Richard Spinney [e], Wei-Ping Hu [f], Liyuan Chai [a,b], Zhihui Yang [a,b], Tiantian Ye [a,b], Ruiyang Xiao [a,b,*]

[a] Institute of Environmental Engineering, School of Metallurgy and Environment, Central South University, Changsha 410083, China
[b] Chinese National Engineering Research Center for Control & Treatment of Heavy Metal Pollution, Changsha 410083, China
[c] Grand Water Research Institute-Rabin Desalination Laboratory, The Wolfson Faculty of Chemical Engineering, Technion-Israel Institute of Technology, Technion City, Haifa 32000, Israel
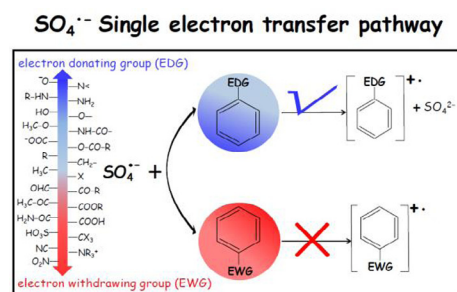[d] Environmental Engineering and Science Program, University of Cincinnati, Cincinnati, OH 45221, USA
[e] Department of Chemistry and Biochemistry, The Ohio State University, Columbus, OH 43210, USA
[f] Department of Chemistry and Biochemistry, National Chung Cheng University, Chia-Yi 62102, Taiwan

HIGHLIGHTS

- We systematically investigated the first step of SET reactions for 76 ACs with SO_4^{-}.
- ΔG°_{SET} decreases with an increase of electron donating character of substituents.
- The calculated k_{SET} for the ACs were compared with their experimental k values.
- We proposed two fundamental SET reaction mechanisms for 76 ACs with SO_4^{-}.

GRAPHICAL ABSTRACT

ABSTRACT

Removal of aromatic contaminants (ACs) in waters by sulfate radical anion (SO_4^{-}) based advanced oxidation technology has been extensively studied. Three main mechanisms have frequently been used to account for the first step of radical oxidation of ACs: radical adduct formation, hydrogen atom abstraction, and single electron transfer (SET), among which the SET pathway is the least understood. In this study, we investigated the first step of SET reactions for 76 ACs with SO_4^{-}. The result shows that the Gibbs free energy (ΔG°_{SET}) of the reaction increases with a decrease of the electron donating character of the substituents on the ACs. The trend was then quantitatively corroborated by a Hammett type plot, indicating that the electrostatic interaction is the driving force for the SET pathway. Further, we compared the calculated second-order rate constants (k_{SET}) for the ACs via the SET pathway with their experimental k values, and proposed two fundamental SET reaction mechanisms based on the identified intermediates. The thermodynamic and kinetic results obtained advance the mechanistic understanding of the SET pathway of radical and non-radical bimolecular reactions, and shed light on the applicability of SO_4^{-} in ACs removal during water treatment processes.

© 2017 Elsevier B.V. All rights reserved.

* Corresponding author at: Institute of Environmental Engineering, School of Metallurgy and Environment, Central South University, Changsha 410083, China.
E-mail address: xiao.53@csu.edu.cn (R. Xiao).
[1] Both Shuang Luo and Zongsu Wei contributed equally to this study.

1. Introduction

Advanced oxidation technologies (AOTs) producing radical species at ambient temperature and pressure have been widely used

to remove aromatic contaminants (ACs) in groundwater, wastewater, and drinking water treatments [1,2]. Hydroxyl radical ($\cdot^-$OH) generated by ozonation, ultraviolet/hydrogen peroxide, or Fenton/photo-Fenton processes, is the most common oxidant species produced in AOTs [3,4]. However, due to its high reactivity toward the ubiquitously present natural organic matters (NOMs), $\cdot^-$OH usually exhibits low removal efficiency of target contaminants in a complex environmental matrix during the AOT process [5,6]. On the contrary, sulfate radical anion-based AOT that produces sulfate radical (SO_4^-) is less affected by the presence of background NOMs due to the selective reactivity of SO_4^-. Consequently, such AOT has received increasing attention for the removal of ACs in the presence of background NOMs in waters [7,8]. In addition, the SO_4^- based *in situ* chemical oxidation (ISCO) technologies also exhibit more practical advantages over other ISCO systems, since the radical precursor salt (*i.e.,* persulfate) are relatively stable and can be delivered for long distances in a subsurface system.

Three main mechanisms have been proposed for the first step of SO_4^- oxidation of ACs: (1) radical adduct formation (RAF), (2) hydrogen atom abstraction (HAA), and (3) single electron transfer (SET) [9–11]. Mounting experimental evidence has confirmed the occurrence of RAF and HAA pathways in SO_4^- oxidation reactions by using electron spin resonance (ESR) spectroscopy [9,12], transient absorption spectroscopy [13], and mass spectrometry [11,14]. In addition, substantial theoretical evidence has been presented to support the radical and non-radical bimolecular reactions via the RAF and HAA pathways on the molecular level. For example, with density functional theory (DFT)-based methods, Caregnato et al. [11] has reported SO_4^- oxidation of gallic acid in RAF and HAA pathways, and experimentally verified the predicted products. They concluded that their DFT calculations in aqueous solution support the formation of phenoxyl radicals via the HAA route for the reactions between phenols and SO_4^-.

Recognizing that the SET reaction is the simplest and fastest of all chemical reactions, experimental identification and description of the SET pathway is, unfortunately, very limited for SO_4^- oxidation reactions [9,15]. The extremely short lifetime of radical cations generated in SET reactions makes it difficult to characterize these reaction intermediates in the presence of other radicals and species [15–17]. For example, Zemel and Fessenden [15] examined the intermediate oxidation products formed within 0.1 and 1 μs for the reactions of SO_4^- with benzene and benzoate derivatives using ESR spectroscopy. By analyzing the phenyl (70%) and hydroxycyclohexadienyl radical (30%) intermediates from the SET reaction products of benzoate radical cation, they concluded that the SET route was the main reaction channel. However, capturing and identifying transient species in the RAF and SET pathways for ACs remains quite an analytical challenge. Tripathi [16] reported that the adduct radicals produced through the RAF route and radical cation via the SET pathway have overlapping absorption signals, resulting in conflicting evidence between the two pathways. More importantly, many questions regarding the mechanisms of the SET reactions of ACs with SO_4^- still remain unanswered. For example, how does one verify the SET pathway and distinguish it from others? How fast does a radical and non-radical bimolecular reaction take place via the SET route? Do the SO_4^- based SET reactions follow certain degradation patterns? The fundamental thermodynamic and kinetic information can be used to predict the byproducts that may be oxidized by SO_4^-. As a reaction proceeds, different degradation pathways lead to different byproducts depending on the reaction mechanisms. With this information available, one can predict the potential byproducts for compounds whose kinetics and thermodynamics have not been experimentally investigated before. Therefore, in addition to further development of analytical techniques, an improved mechanistic understanding of the SET reaction of ACs with SO_4^- is desired.

Quantum mechanics-based calculation offers an alternative way to provide mechanistic insights into radical oxidation, especially when the experimental identification is technically challenging. For instance, Madhavan et al. [18] investigated the ·OH-mediated degradation byproducts for ibuprofen with electrospray ionization mass spectrometry, and mono and dihydroxylated intermediates, such as 2-(4-(1-hydroxy-2-methylpropyl) phenyl) propanoic acid, were identified as secondary and tertiary byproducts. However, their evidence was insufficient to identify the reaction pathways on the molecular level. Upon the Madhavan et al. [18] study, Xiao et al. [19] investigated ·OH oxidation of ibuprofen in a variety of pathways, and constructed the energy profiles for these reaction channels with DFT calculation. They elucidated the reaction mechanisms and confirmed that the first and dominant step of ibuprofen oxidation with ·OH is to undergo the HAA channel, which is followed by an additional ·OH attack with the resulting ibuprofen radical, forming the observed mono and dihydroxylated intermediates. Their quantum mechanics-based calculations supported the experimental evidence obtained by Madhavan et al. [19]. Further, previous studies have revealed that the overall reactivity for SO_4^- is strongly dependent on electron donating/withdrawing character of functional groups on the organic compounds [20]. Xiao et al. [8] reported that the overall SO_4^- reactivity dependence can be quantitatively described by quantum mechanics-based descriptors such as energies of the highest/lowest occupied molecular orbitals. Our previous study points to a necessity to investigate the electronic effect of functional groups on SO_4^- based SET reactions.

In the present study, we selected 76 ACs covering a wide variety of structural diversities and reactivities with SO_4^-. We performed a quantum mechanical study on the feasibility of these contaminants taking the SET pathway in SO_4^- oxidation reactions. We tested the hypothesis that, the electron donating/withdrawing character of the functional groups affects the thermodynamic viability of the SET reaction. In addition, the kinetics of the ACs that are thermodynamically feasible to react with SO_4^- via the SET channel were also investigated with the emphasis on the connection between the calculation results and experimental measurements. Specifically, we compared the calculated SET rate constants (k_{SET}) with the observed second-order values (k_{obs}), and proposed two fundamental SET reaction mechanisms based on the identified intermediates.

2. Materials and methods

2.1. Aromatic contaminants

In the present study, 40 benzene and 36 benzoate derivatives, totaling 76 ACs, were investigated, and their structures are listed in Table A1 in Appendix A. The selection of these ACs is based on the environmental relevance, existing studies, structural diversity in functional groups, and data for both conjugate acid–base pairs for acidic/basic species. The singly charged states were also considered for compounds containing hydroxyl group (−OH), carboxyl group (−COOH), secondary (−NH−) and tertiary amine (−N<) group. Their pK_a values are listed in Table A2.

2.2. Electronic structure calculations

Due to the intractable amount of time required for *ab initio* conformational searching, the global minimum was sought using Spartan'10 with the Merck Molecular Force Field (MMFF) [21]. The MMFF was designed for modeling organic molecules so is well suited for this task [21]. The lowest energy conformer of a compound from Spartan was then optimized at the DFT level using Gaussian

09 (Revision C.01) to determine the global minimum conformation for each compound [22]. The geometry optimizations and vibrational frequencies of all the reactants and products were calculated using the hybrid density functional theory at M06-2X/6-311++G** and B3LYP/6-311++G** levels [23,24]. The M06-2X has been the recommended functional to investigate the thermodynamics and kinetics for radical-molecule reactions, and it has been widely used in calculating single electron transfer reactions [24,29,32]. For example, Iuga et al. [32] conducted a quantum mechanics-based kinetic study on the reactivity of phenothiazine (PTZ) with ·OH and hydroperoxyl radical (HO$_2^-$) at M06-2X/6-311++G** level in conjunction with the solvation model of density (SMD) through the SET route. Their results showed that M06-2X yields excellent results compared to experiments. The B3LYP functional was also used and compared with M06-2X, as B3LYP has been shown to give reliable results for radical oxidation of organic molecules [17,33]. The method for the frequency calculation was set by the method used for the geometry optimization (*i.e.,* M06-2X/6-311++G** in this study). In order to mimic water environment, the solvent effect was included with the SMD approach [25,26]. The SMD model calculates $\Delta G°_{solvation}$ from the gas-phase to a solvent taking into account both the electrostatic and the cavitation dispersion energies, and the model has been successfully applied for the aqueous phase free energy [27–29]. It is considered to be a reliable solvation model due to its applicability to both charged and uncharged solutes in water [25,26]. Further, Truhlar and coworkers indicated that the experimental solvation free energies and calculated values using SMD model showed good agreement for a large number of compounds [30]. More importantly, in the current study, we are more interested in the reaction energies, thus using the accurate SMD model to obtain the energies of the products AC radical cation and SO$_4^{2-}$ relative to the reactants AC and SO$_4^-$ was justified. The thermal contributions to enthalpy, free energy, and electrostatic potential were also calculated at the same levels of theory as mentioned above [31]. The determination of the thermodynamic parameters, such as enthalpies ($\Delta H°_{SET}$) and $\Delta G°_{SET}$ at 298 K, were detailed in our previous study [31].

2.3. Marcus theory

Marcus theory has been used to investigate the kinetics for the SET reaction pathway for radical and non-radical bimolecular reactions [34,35]. Galano and other pioneering scientists recommended Marcus theory to estimate reaction processes involving electron transfer, as it can provide quick and reasonable results as compared to experimental measurements [29]. For example, in the study by Iuga et al. [32], Marcus theory was used to construct the SET energy profiles for the reactions of PTZ with ·OH and HO$_2^-$. In the theory, the rate of electron transfer reaction depends on the distance between electron donor and acceptor, reaction free energy change and the energy for reorganized reactants and surrounding solvent [36,37]. The activation barrier ($\Delta^\ddagger G°_{SET}$) was defined as:

$$\Delta^\ddagger G°_{SET} = \frac{(\lambda + \Delta G°_{SET})^2}{4\lambda} \tag{1}$$

$$\lambda = \Delta E°_{SET} - \Delta G°_{SET} \tag{2}$$

where $\Delta G°_{SET}$ is the free energy of single electron transfer reaction, λ is the reorganization energy, which is a measure of the free-energy change associated with solute and solvent rearrangements, and $\Delta E°_{SET}$ is the energy difference of corrected energy between reactants ($\Delta E°_{reactants}$) and vertical products ($\Delta E°_{vertical\ products}$) involving a change of charge and spin multiplicity at the same geometries.

$$\Delta E°_{SET} = \Delta E°_{vertical\ products} - \Delta E°_{reactants} \tag{3}$$

While Marcus theory provides a straightforward method to determine the energy changes for the SET processes, the solvent effects which are difficult to model explicitly may make very important contribution to the energy changes. This is especially true for the SET process in aqueous solution, since the neutral AC molecule becomes a radical cation and the radical reactant changes from an anionic radical (SO$_4^-$) to dianionic species. The changes in charge states would cause large reorganization and solvation energies. While the SMD solvation model was used for the solvent effects, solvent reorganization cannot be modeled explicitly by any continuum solvation model. In addition, quantum tunneling effects should also be considered in more rigorous treatment, but they were not taken into account explicitly in the current study to simplify the calculation.

2.4. k_{SET} calculations

The calculation of k_{SET} for the ACs that are thermodynamically feasible with SO$_4^-$ via the SET pathway was performed with the conventional transition state theory (TST), which is detailed in previous studies [31,35]. The method using Marcus theory in conjunction with conventional TST for k_{SET} has been proved to be a reliable and excellent predictive approach, and the methodological uncertainty is less than the experimental uncertainty [29]. First, k_{act}, the rate constants determined with activation energy barrier heights, was calculated using conventional TST at 1 M standard state:

$$k_{act} = l\Gamma(T)\frac{k_B T}{h} \exp\left(\frac{\Delta^\ddagger G°_{SET}}{RT}\right) \tag{4}$$

where l is the reaction path degeneracy accounting for the number of equivalent reaction paths ($l = 1$ for the SET reaction); T is temperature (298 K in this study); $\Gamma(T)$, a temperature-dependent factor, corresponds to quantum mechanical tunneling and is approximated by Eckart's approach; k_B is Boltzmann's constant, h is Planck's constant, and R is gas constant. The k_{act} values are reported to be close to the diffusion limit due to their low energy barriers. Thus, with the assumption that the reaction occurs within a specific distance, Collins–Kimball theory was used to correct for the diffusion limit:

$$k_{SET} = \frac{k_D k_{act}}{k_D + k_{act}} \tag{5}$$

where k_D is the diffusion-limited rate constants. Smoluchowski equation was used to calculate k_D, which is detailed elsewhere [17,28].

Recently, Tratnyek and coworkers nicely detailed the Marcus–Eberson method (*i.e.,* the collide- and -react model) for k_{SET}, which is calculated as [38,39]:

$$\log k_{SET.ME} = \log k_d - \log\left\{1 + 0.1 \times \exp\left\{W + \left[\frac{\lambda}{4}\left(1 + \frac{\Delta G°'}{\lambda}\right)^2\right]/0.592\right\}\right\} \tag{6}$$

where k_d is the diffusion rate for electron donor and acceptor diffusing together and forming the precursor complex, assumed to be $10^{10}\ M^{-1}\ s^{-1}$, and $\Delta G°'$ is the corrected standard free energy of the reaction:

$$\Delta G°' = \Delta G° + (Z_1 - Z_2 - 1)\frac{e^2 f}{Dr} \tag{7}$$

where Z_1 and Z_2 are charges on the electron acceptor and donor species, in our study for neutral benzene derivatives $Z_1 - Z_2 = -1$, for -1 charged benzoates derivatives $Z_1 - Z_2 = 0$, and for -2 charged

benzoates derivatives $Z_1 - Z_2 = 1$. e is electronic charge ($e^2 = 331.2$), f is ionic effect factor (when ionic strength = 0, $f = 1$ unitless), D is dielectric constant ($D_{water} = 78.5$ unitless), and r is the distance between the centers of the spheres with the assumptions that the two reactants are spherical and outer sphere electron transfer occurs ($r = 6$ Å). W can be calculated as:

$$W = \frac{331.2 \times Z_1 Z_2 f}{D \times r} \tag{8}$$

In Eqs. (7) and (8), r is from the literature [39]. Eberson [39] used 6 Å for $Fe(CN)_6^{3-}$ reacting with neutral organic molecules. Eberson also used 4 Å for r in Marcus model training. In fact, this number can be approximately taken to be $r_1 + r_2$. We calculated the radius of SO_4^- and 36 target aromatic contaminants that are thermodynamically feasible with SO_4^- at SMD/M06-2X/6-311++G**. The radius for SO_4^- is 2.6 Å. We tabulated r (i.e., $r_1 + r_2$) for 36 ACs that are thermodynamically favorable with SO_4^- in Table A3. The average r values for 36 ACs are 6.09 Å. Thus, based on our calculation, 6 Å is a reasonable number. In general, the Marcus–Eberson method is similar to Marcus-conventional TST method, as both methods are based on the Eyring equations but with different parameterization. We also included the Marcus–Eberson method for k_{SET} calculation for comparison purpose.

It is noted that the proper way to calculate the tunneling effect should include the solvation effects along the reaction path by using the variational transition state theory with multidimensional tunneling (VTST/MT) method. But the VTST/MT calculations are very complicated and resource-demanding, we neglected the effects and concentrated on the trends obtained in the current study. As for the methods we used (i.e., Marcus–Eberson method and Marcus-conventional TST), they gave a good order-of-magnitude estimate for the k_{SET} values. The Eckart function might be a reasonable approximation to the potential profile along the reaction path in the gas phase. In solution, the solvation effect is different at different molecular geometries on the reaction path. Thus it is not correct to assume the energy profile still resembles the Eckart function. However, it is expected that the tunneling effect should not be large due to the low barriers. In addition, in our study only the relative energies of reactions or the relative rate constants are important. The absolute values of rate constants are not very crucial. Accurate rate constant calculation should be done with VTST/MT and a more sophisticated collision-rate model. We believed that although the calculated k_{SET} are approximated values, this result could shed light on k_{SET} calculation for future research.

3. Results and discussion

3.1. Thermodynamics for the SET reaction

3.1.1. Thermodynamic feasibility

The results of enthalpy change (ΔH_{SET}°), Gibbs free energies (ΔG_{SET}°), entropy (ΔS_{SET}°), reorganization energy (λ) and Gibbs free energies of activation ($\Delta^{\ddagger}G_{SET}^\circ$) calculated at SMD/M06-2X/6-311++G** level of theory for SO_4^- with 40 benzene derivatives and 36 benzoate derivatives via the SET pathway are listed in Tables A4 and A5. The SET pathway for 36 out of 76 ACs is thermodynamically favorable, ranging from −44.0 to −0.39 kcal mol^{-1}. These 36 compounds typically contain electron donating groups, such as −NH$_2$, −NH−, −NH<, −O−, −O−CH$_3$, −OH, and −O$^-$. The results calculated at SMD/B3LYP/6-311++G** level of theory were tabulated in Tables A6 and A7. The distribution of ΔG_{SET}° for the SET reaction between ACs and SO_4^- was shown in Fig. A1. Both the M06-2X and B3LYP calculations give similar results, but on average the ΔG_{SET}° values calcu-

lated with B3LYP functional are approximately 0.8 kcal mol^{-1} higher. For the rest 40 out of 76 ACs, the ΔG_{SET}° values range from 0.12 (o-bromobenzoate) to 24.9 kcal mol^{-1} (p-nitrobenzoic acid) at SMD/M06-2X/6-311++G** level of theory (Tables A4 and A5). These compounds typically contain electron withdrawing groups, such as −NO$_2$, −Br, and −CN. However, k_{obs} values for benzonitrile ($\Delta G_{SET}^\circ = 16.2$ kcal mol^{-1}), benzoic acid ($\Delta G_{SET}^\circ = 13.7$ kcal mol^{-1}, and o-bromobenzoic acid ($\Delta G_{SET}^\circ = 13.7$ kcal mol^{-1}) are 1.2×10^8, 1.2×10^9, and 8.7×10^8 M^{-1} s^{-1}, respectively, indicating that other reaction mechanisms such as RAF and HAA are dominant for these compounds [10].

Wang et al. [40] studied the decomposition process of anthracene (ANT), a typical prioritized controlled polycyclic aromatic hydrocarbon, in aqueous phase reacting with SO_4^- by the transition state theory. They reported that at PCM/BHandHLYP/6-31G* level, the initial one–electron transfer step from ANT to SO_4^- has a negative energy barrier (−19.7 kcal mol^{-1}), indicating that SET is the dominant reaction route. Our results also show that the SET reaction is thermodynamically favorable for ANT with ΔG_{SET}°=−21.5 kcal mol^{-1} by the M06-2X calculation, which is in agreement with their study. Interestingly, their results showed that SO_4^- actually reacts with ANT via a radical addition pathway with formation of a 1.47 Å bond between ANT molecule and SO_4^-. Thus, although they assumed the SET reaction, the evidence provided by Wang et al. [40] does not seem to be strong enough to support that the reaction of ANT and SO_4^- is via SET pathway.

There are several experimental studies suggesting that the main reaction between ACs and SO_4^- takes place by an initial electron transfer from the aromatic ring to the radical anion. Neta and other pioneering scientists determined the bimolecular rate constants $k_{SO_4^-}$ values for a variety of ACs by irradiating persulfate solution with pulsed radiolysis [10,12]. Neta et al. [10] investigated 21 different benzene and benzoate derivatives, and related the $k_{SO_4^-}$ values to σ in a Hammett type plot, which describes a linear free-energy relationship relating radical reactivities and the structural features for benzene/benzoate derivatives. Their results showed that SO_4^- yields a ρ value of −2.4 for both substituted benzenes and benzoates, where ρ is the slope of the Hammett plot and it reflects the sensitivity of a reaction to the electronic effect of the substituents. It is noted that the substituent effects on these rate constants show the ρ values for $\cdot^-OH$ and hydrated electron (e_{aq}^-) are −0.5 and −4.8, respectively. Since the $\rho_{SO_4^-}$ is about 5 times greater than $\rho_{\cdot OH}$, and is very similar to $\rho_{e_{aq}^-}$ (i.e., arctan (−2.4) ≈ arctan (−4.8)), they concluded that SO_4^- most likely reacts with ACs by a single electron transfer mechanism [10]. However, in the SET reaction of a compound with SO_4^- and e_{aq}^-, SO_4^- is an electron acceptor forming SO_4^{2-}, while e_{aq}^- is an electron donor. The opposite redox behavior of both species indicates that direct comparison of $\rho_{SO_4^-}$ and $\rho_{e_{aq}^-}$ may not be appropriate. Further, they proposed that benzene reacts with SO_4 forming a radical cation first, which then reacts with water to form hydroxycyclohexadienyl radical [15]. Although hydroxycyclohexadienyl radical was observed with the ESR spectra, it cannot be viewed as convincing evidence supporting that the reaction forms a radical cation first by SO_4^-. Moreover, our calculations indicate that the reaction of SO_4^- with benzene through SET route is not thermodynamically favorable with ΔG_{SET}° of 10.4 and 7.62 kcal mol^{-1} at B3LYP and M06-2X levels, respectively. Zemel et al. [15] investigated the SET products for the reaction of SO_4^- with p-hydroxybenzoate by ESR spectroscopy. They suggested that p-hydroxybenzoate initially reacts with SO_4^- via SET route forming p-hydroxybenzoate radical cation which then becomes p-oxidobenzoate radical in water via the HAA pathway. Although in their study the radical cation was not directly

observed, our calculation predicted the first step ΔG°_{SET} of -7.96 and -7.88 kcal mol^{-1} at B3LYP and M06-2X levels, respectively, which supports their proposed mechanism.
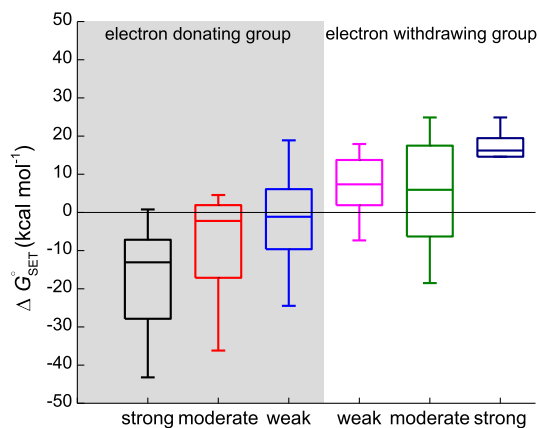
3.1.2. Solvation effect

The solvation effect plays a significant role in determining the inner/outer solvent shells activation energies and the rearrangement barriers in the SET reactions [41,42]. A reaction is thermodynamically favored in the medium which favors the association of reactants. In fact, the SET reaction in gas phase is intrinsically endothermic because of the charge separation. We calculated the gas-phase ΔG°_{SET} values for the ACs that are thermodynamically favorable in water, and the result shows that none of the reactions would occur in the gas phase (data not shown). In the study by Caregnato et al. [11], the reported gas-phase ΔG°_{SET} values of the oxidation of gallic acid and gallate by SO$_4^{\cdot-}$ are 223 and 115 kcal mol^{-1}, respectively, indicating the reactions are not thermodynamically favorable. Our ΔG°_{SET} values for gallic acid and gallate in the aqueous solution are -7.17 and -13.0 kcal mol^{-1} by M06-2X calculation and -4.53 and -12.5 kcal mol^{-1} by B3LYP calculation, respectively. The result indicates that strong solvation favors the formation of the dianions in polar solvents, and thus may promote the SET pathways.

3.2. Electron donating/withdrawing properties of functional groups

Xiao et al. [8] conducted a meta-analysis to understand the role of functional groups on the reactivity between SO$_4^{\cdot-}$ and trace organic contaminants. They found that the contaminants which are dominated by electron transfer reactions tend to exhibit faster second-order rate constants than other pathways. In light of the previous results, we hypothesized that an AC compound with electron donating group(s) is more likely to react by the simplest and fastest route, the SET pathway.

To test this hypothesis, we systematically investigated the role of electron donating/withdrawing functional groups on the SET reactions. We categorized all 76 ACs into 26 different functional groups. First, all the compounds were grouped into either electron–donating or electron-withdrawing groups. Then, within a group the compounds were further classified as having strongly, moderately or weakly electron donating (or withdrawing) groups (Table A8). For example, the hydroxyl group is a strong electron-donating group, while a nitro group is a strong electron-withdrawing group. We plotted the feasibility of the SET pathway between SO$_4^{\cdot-}$ and all ACs (i.e., ΔG°_{SET}) against their functional groups. Fig. 1 shows a clear relationship between ΔG°_{SET} and the electron donating/withdrawing ability of the substituents. The median ΔG°_{SET} values increase from the strong electron donating groups to strong withdrawing groups. Thus, a compound with electron-donating groups is more likely to react through the SET channel than that with electron–withdrawing groups.
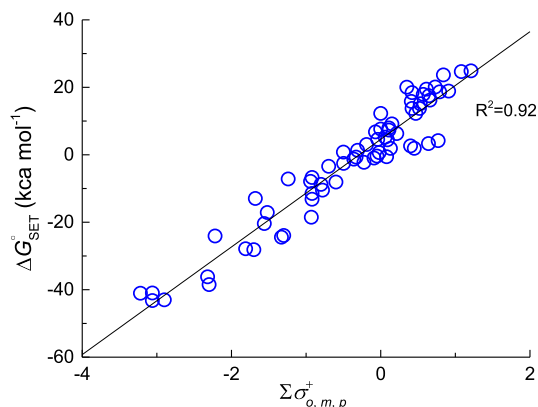
The ACs that only contain electron-withdrawing groups cannot spontaneously react with SO$_4^{\cdot-}$ via the SET route. For example, benzaldehyde (–CHO group) and benzoic acid (–COOH groups) reactions with SO$_4^{\cdot-}$ are not thermodynamically favorable to take place via the SET pathway with ΔG°_{SET} values of 20.1 and 13.7 kcal mol^{-1} at M06-2X level, respectively. But for ACs containing both strong electron-donating and electron-withdrawing groups, it seems that the former out-competes the latter for most ACs in the SET reactions. For example, in p–methoxybenzaldehyde (–CHO and –O─CH$_3$) and m-aminobenzoic acid (–COOH and –NH$_2$), both types of functional groups are present, and the calculated ΔG°_{SET} values are -0.39 and -18.5 kcal mol^{-1}, respectively at M06-2X level. This is similar to the electrophilic aromatic substitution reactions where the electron-donating group dominates

Fig. 1. Box plot of ΔG°_{SET} for SO$_4^{\cdot-}$ oxidation of aromatic contaminants (ACs) through the SET pathway. The selected 76 ACs are categorized by the electron donating/withdrawing properties of the respective functional groups. The grey area indicates the electron donating groups, while the white area shows the electron withdrawing groups. A compound containing multiple functional groups is counted in the stack for each functional group present. The strong electron donating group (black) includes oxide, tertiary amine, secondary amine, amino, hydroxyl, ether and methoxy; moderate (red), aminoacyl, carboxylate, and acetoxy; weak (blue), alkyl, methylene, methyl, and phenyl. For electron withdrawing group, halogen is the weak withdrawing group (pink); moderate (green), formyl, carbonyl group, acyl, amide, carboxylic acid, and sulfonic acid; strong (dark blue), trifluoromethyl, cyano, quaternary amine and nitro. (For interpretation of the references to colour in this figure legend, the reader is referred to the web version of this article.)
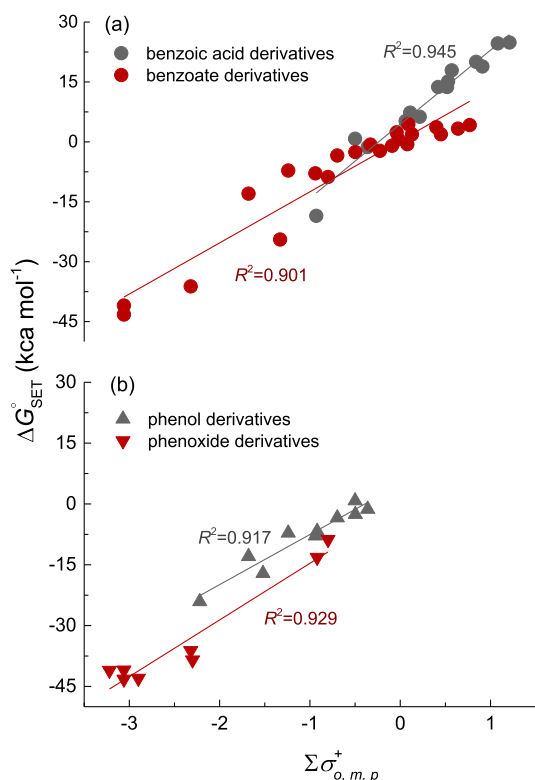
over electron-withdrawing groups in ring activation and directing effects.

In order to quantify the effect of the electronic properties of substituents on the SET reactions, Hammett substituent constants (σ) were plotted against the ΔG°_{SET} values to explore any relationship. We found that the σ^+ yields the best correlation coefficient ($R^2 = 0.92$) as compared to σ ($R^2 = 0.66$) and σ^- ($R^2 = 0.86$), where σ^+ reflects the delocalization of a positive charge, and σ^- reflects delocalized conjugated negative charge. Fig. 2 shows the increasing trend of ΔG°_{SET} as function of σ^+, corroborating that the electronic properties of the substituent exerts a profound impact on the probability of the radical taking the SET pathway. The Hammett σ^+ values were developed to deal with reactions where a positive charge is produced, specifically for benzylic carbocations or aromatic cations generated in electrophilic aromatic substitution reactions. While the SET does not match these processes exactly, it does produce an aromatic radical cation. Interestingly, the dissociated and neutral forms of benzoic acid and phenol derivatives exhibit different Hammett distribution pattern with SO$_4^{\cdot-}$. Fig. 3 illustrates that the benzoate and phenoxide derivatives generally lie lower than the neutral forms, indicating that the deprotonated species are more reactive with SO$_4^{\cdot-}$ through the SET reaction pathway than their neutral forms. In the case of benzoates this is likely due to the rapid radical decarboxylation of the carboxylate group. For example, the distribution of highest occupied molecular orbital (HOMO) for o-toluic acid does not include the carboxylic acid group. However, the distribution HOMO on o-toluiate includes the carboxylate group (Fig. A2). This HOMO distribution indicates that the carboxylate group can easily be attacked by SO$_4^{\cdot-}$, which would lead to rapid decarboxylation and to the generation of aromatic radical. This is also true for m-toluic acid/m-toluate, p-toluic acid/p-toluate, benzoic acid/benzoate, and p-terephthalic acid/p-carboxybenzoate (Fig. A2). It should be noted that if the reactions of SO$_4^{\cdot-}$ with ACs containing a carboxylic acid are thermodynamically feasible via SET (i.e. it also has a moderate to strong electron donating group), we did observe that the distribution of HOMO covers the carboxylic acid group, such as p-hydroxybenzoic acid/p-hydroxybenzoate, gallic acid/galliate, m-aminobenzoic
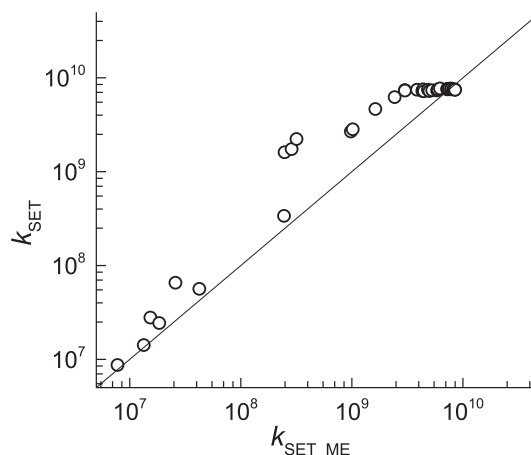
Fig. 2. The relationship of $\sum \sigma_{o,m,p}^+$ and ΔG_{SET}° for the SET reactions of the ACs and SO_4^-. $\sum \sigma_{o,m,p}^+$ is the sum of σ^+ at different positions on the benzene ring. For example, 3,5-dihydroxy-4-oxidobenzoate is consisted of one carboxylic acid group (–COO⁻), one oxide group (–O⁻), two hydroxyl groups (–OH). Thus, $\sum \sigma_{o,m,p}^+ = \sigma_p^+(-COO^-) + \sigma_p^+(-O^-) + 2 \times \sigma_m^+(-OH) = (-0.02) + (-2.3) + 2 \times (-0.37) = -3.06$. The series of σ data (*i.e.*, σ^-, σ^+, and σ) at different positions (*i.e.*, meta-, ortho-, para-) were documented in previous studies [49–51].

acid/*m*-aminobenzoate, 4-methylsalicylic/4-methylsalicylate, and *p*-methoxybenzoic acid/*p*-methoxybenzoate (Fig. A2). However, if an electron withdrawing group is also present on the AC molecule (*e.g.*, *p*-acetylbenzoic acid/*p*-acetylbenzoate, *p*-chlorobenzoic acid/*p*-chlorobenzoate, *p*-nitrobenzoic acid/*p*-nitrobenzoate, *o*-bromobenzoic acid/*o*-bromobenzoate, *p*-cyanobenzoic acid/*p*-cyanobenzoate, and *p*-bromobenzoic acid/*p*-bromobenzoate), the thermodynamic feasibility is dominated by the electron withdrawing group(s) (*i.e.*, they are not reactive), regardless of presence of –COOH/–COO– group (Fig. A2). In this case, the distribution of HOMO for these compounds does not reflect any reactivity, and thermodynamic feasibility should be calculated based on Hess' law.
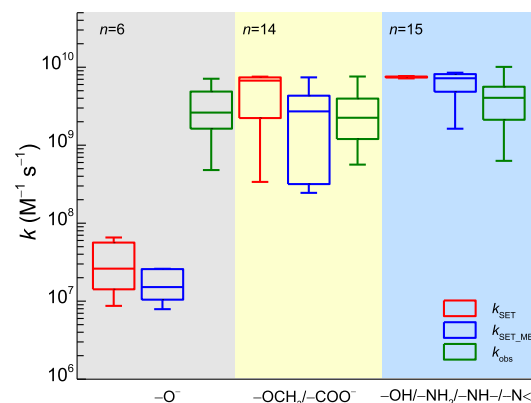

Fig. 3. The relationship of $\sum \sigma_{o,m,p}^+$ and ΔG_{SET}° for the SET reactions of benzoic acid/benzoate derivatives (a) and phenol/phenoxide derivatives (b) with SO_4^-.

Fig. 4. Comparison of k_{SET} with the k_{SET_ME} using the Marcus–Eberson method.

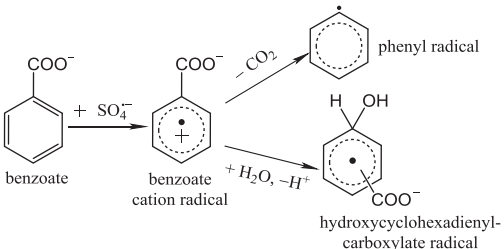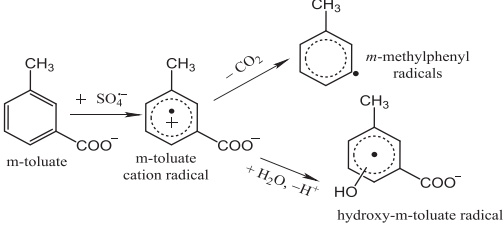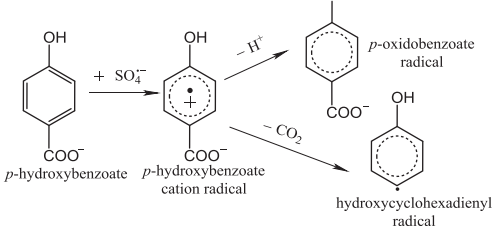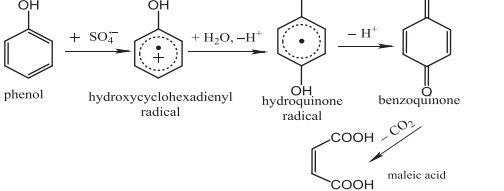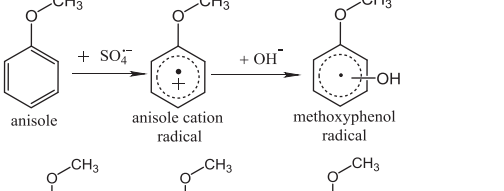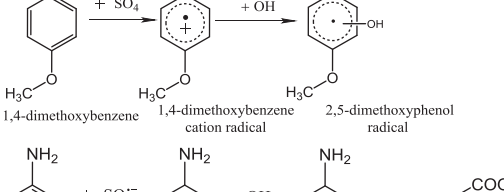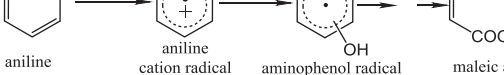Since the effect of electron donating/withdrawing ability of the functional groups on ΔG_{SET}° can be quantified by Hammett constants (Fig. 2), we expected a similar correlation between the electronic effect of the functional groups and $\Delta^\ddagger G_{SET}^\circ$ for the ACs that are thermodynamically feasible to react with SO_4^-. We limited our investigation to these compounds because it is only meaningful to study the kinetics when the reactions are thermodynamically feasible. However, Figs. A3 and A4 illustrate that the effect of electron donating ability of the functional group on $\Delta^\ddagger G_{SET}^\circ$ is not obvious, and the trend cannot be quantified by various Hammett constants. This is in fact not surprising, since Hammett constants were developed with respect to the equilibrium constants, and hence they are more applicable to ΔG_{SET}°. The lack of correlation to $\Delta^\ddagger G_{SET}^\circ$ may be attributed to the means in which $\Delta^\ddagger G_{SET}^\circ$ was calculated (see Eqs. (1) and (2)) and/or the "early" arrival of transition state (TS) of SET reaction. The solvent effect is difficult to calculate and so an approximation was used. The TS structure is more similar to the reactants than to the products. Reactions with "early" TS would have barriers not correlate strongly with the energies of reactions since it looks more like the reactants. These likely introduce errors into the $\Delta^\ddagger G_{SET}^\circ$, obfuscating any possible correlation with Hammett constants.

The classification of functional groups based on electron donating/withdrawing does not explicitly reveal whether the SET reaction occurs in benzene ring or its substituent, although several previous studies implied that the reaction takes place by an electron transfer from the benzene ring to SO_4^- [9,10,12,15]. In order

Fig. 5. Comparison of our calculated k_{SET} values, the k_{SET_ME} values by the Marcus–Eberson method, and the experimental k_{obs} values for 35 ACs that are thermodynamically feasible to react with SO_4^- through the SET pathway by functional group. Anthracene is not included, as it does not belong to any group listed.

Table 1
Reaction pathways for the ACs and SO_4^- through the SET pathway.

ACs	Reaction pathways	Reference
Benzoate	benzoate $+ SO_4^{\cdot-}$ → benzoate cation radical $\xrightarrow{-CO_2}$ phenyl radical; benzoate cation radical $\xrightarrow{+ H_2O, -H^+}$ hydroxycyclohexadienyl-carboxylate radical	[15]
m-toluate	m-toluate $+ SO_4^{\cdot-}$ → m-toluate cation radical $\xrightarrow{-CO_2}$ *m*-methylphenyl radicals; m-toluate cation radical $\xrightarrow{+ H_2O, -H^+}$ hydroxy-m-toluate radical	[15]
p-hydroxybenzoate	p-hydroxybenzoate $+ SO_4^{\cdot-}$ → p-hydroxybenzoate cation radical $\xrightarrow{-H^+}$ *p*-oxidobenzoate radical; p-hydroxybenzoate cation radical $\xrightarrow{-CO_2}$ hydroxycyclohexadienyl radical	[15]
Phenol	phenol $+ SO_4^{\cdot-}$ → hydroxycyclohexadienyl radical $\xrightarrow{+ H_2O, -H^+}$ hydroquinone radical $\xrightarrow{-H^+}$ benzoquinone $\xrightarrow{-CO_2}$ maleic acid	[46]
Anisole	anisole $+ SO_4^{\cdot-}$ → anisole cation radical $\xrightarrow{+ OH^-}$ methoxyphenol radical	[47]
1,4-Dimethoxybenzene	1,4-dimethoxybenzene $+ SO_4^{\cdot-}$ → 1,4-dimethoxybenzene cation radical $\xrightarrow{+ OH^-}$ 2,5-dimethoxyphenol radical	[12]
Aniline	aniline $+ SO_4^{\cdot-}$ → aniline cation radical $\xrightarrow{+ OH^-}$ aminophenol radical → maleic acid	[48]

to localize the atom or group at which the SET reaction occurs, we calculated the electrostatic potential (ESP) partial atomic charge on the carbon and hydrogen atoms in the aromatic ring for all the ACs [43,44]. If the SET reaction occurs by transferring an electron from the ring, it is expected that the higher the ESP negative charge in the ring (*i.e.*, the higher the electron density in the ring), the more readily that the SET reaction occurs. Our results

do not support this expectation. Fig. A5 shows that there is no clear pattern for ΔG_{SET}° and the total ESP charge on carbon and hydrogen atoms in the ring structure. For instance, dimethyl phthalate (grey dot in Fig. A5) does not react with SO_4^- with ΔG_{SET}° of 17.5 kcal mol^{-1} at M06-2X level, but the total ESP charge in the ring structure is −0.26 a.u. On the other hand, gallic acid (grey dot in Fig. A5) reacts spontaneously with SO_4^- with ΔG_{SET}° of

−7.17 kcal mol^{-1}, but the total ESP charge in the ring structure is 0.44 a.u. The results show that the SET reaction for the selected 76 ACs is not correlated to the total ring charge, indicating that the electron transfer does not always occur from the benzene ring.

3.3. Kinetics and mechanisms for the SET reaction

3.3.1. Kinetics

The k_{SET} values for 36 ACs that are thermodynamically favorable with SO_4^- through the SET pathway were calculated and compared with the k_{obs} (Table A9). Since the reaction barriers ($\Delta^{\ddagger}G^{\circ}_{SET}$) involving electron transfer are low with a mean of 2.95 kcal mol^{-1} (Tables A4–A7), all the k_{SET} values calculated using conventional TST were corrected for the diffusion limit. Table A9 shows that for 29 out 36 ACs, their k_{SET} values are on the same order of magnitude with their k_{obs} ($\sim10^9$ M^{-1} s^{-1}), indicating that with the exception of ACs with oxide group, as long as the SET pathway between ACs and SO_4^- is thermodynamically plausible, the SET pathway mainly contributes to their overall SO_4^- reactivity. The k_{SET} was then plotted against k_{obs} to examine any relationship. As Fig. A6 illustrates, there is no relationship between these two rate constants, which is expected to some extent. The overall reaction rate constants between ACs and SO_4^- depend not only SET pathway, but also other reaction channels, such as HAA and RAF pathways. In fact, the HAA and RAF channels may always compete with the SET pathway, resulting in no specific relationship between k_{SET} and k_{obs} values. In addition, these k_{SET} values were compared with the k_{SET_ME} using the Marcus–Eberson method. Fig. 4 shows that the k_{SET} values yielded by these two discrete methods are in a good agreement, suggesting that both methods are valid for k_{SET} calculation.

Since the effect of electron donating/withdrawing ability of the functional groups on ΔG°_{SET} can be quantified by σ constants (Fig. 2), we expected similar electronic effects of the functional groups on k_{SET} and k_{obs}. However, Figs. A7 and A8 show that there is lack of correlation between various σ constants (i.e., σ, σ^+, or σ^-) and k_{obs}/k_{SET}, suggesting that the electronic effect of the functional groups does not necessarily exert influence on kinetics for the ACs with a wide spectrum of functional groups. But our result implicitly illustrates that for certain functional group(s) the electronic effect does exhibit impact on k_{SET} (Fig. 5). For instance, the oxide group (–O$^-$) is a strong electron donating group. The k_{SET} values for the six compounds that have oxide group (3, 5-dihydroxy-4-oxidobenzoate, phenoxide, m-aminophenoxide, 4-acetamidophenolate, 4-methyl-2-oxidobenzoate, and p-oxidobenzoate) are the slowest (on the order of 10^7 M^{-1} s^{-1}), indicating that the contribution of SET pathway was insignificant to the overall reaction. We suspected that the electronic charge repulsion and strong solvation may reduce the kinetics for the reaction between compounds with oxide group and SO_4^- [45]. The corrected Gibbs free energy (i.e., $G^{o'}$) in Eq. (7) depends on the charges of the two species. Since the charges on the ACs and SO_4^- are both negative, it could decrease the reaction rate, as the molecules repel each other. In addition, the localized charge on the single oxygen atom should make it form multiple stronger hydrogen bonds to water, as compared to a carboxylate group. This may form a stronger solvation cage, inhibiting their reactions with SO_4^- [45]. In contrast, other compounds containing strong electron donating groups, such as –OH, –N<, –NH–, and –NH$_2$, behave differently. Their k_{SET} values are very close to the diffusion limit, indicating that the SET pathway accounts for the majority of k_{obs}. Compounds that have moderate electron donating groups such as carboxylate (–COO$^-$ and –OCH$_3$) do not follow any pattern, and their k_{SET} can be either fast (e.g., gallate) or slow (e.g., p-oxidobenzoate). Based on the results, it is concluded that the SET contribution in total SO_4^- oxidation

kinetics of ACs partially depends on electron donating abilities of functional groups.

3.3.2. Reaction mechanisms

Reaction mechanisms and patterns for seven ACs (namely, benzoate, m-toluate, p-hydroxybenzoate, phenol, anisole, 1,4-dimethoxybenzene, and aniline) and SO_4^- via the SET route are summarized in Table 1. We selected these compounds because their SET reaction intermediates have been identified [12,15, 46–48]. More importantly, the existence of these observed intermediates corroborates our calculations on the electronic effect of the substituents on thermodynamic feasibility. For example, Olmez–Hanci and Arslan–Alaton [46] reported that phenol, an aromatic compound with a strong electron donating group (i.e., –OH), first reacts with SO_4^- forming phenol radical cation. In fact, these seven ACs can be all categorized into either strong (black box) or moderate (red box) electron donating group in Fig. 1.

Based on the identified reaction intermediates, two fundamental SET processes were proposed. The first is the decarboxylation of benzoate compounds (e.g., benzoate, m-toluate, and p-hydroxybenzoate). This occurs via a single electron transfer from the carboxylate group to the SO_4^- producing SO_4^{2-} and a benzoate (carboxylate) radical which then rapidly dissociate to a neutral CO_2 molecule and a phenyl radical. The second mechanism is a SET from the aromatic ring generating a phenyl radical cation (e.g., phenol, anisole, 1,4-dimethoxybenzene, and aniline in Table 1). The phenyl radical cation can then undergo several different reactions, depending on the nature of existing substituents. In general, these radical cation can react with water (or hydroxide) via a "nucleophilic attack" adding a hydroxyl group to the ring and producing a hydroxycyclohexadienylcarboxylate radical, hydroquinone radical, methoxyphenol radical, 2,5-dimethoxyphenol radical, aminophenol radical, hydroxyl-m-toluate radical, or cyclohexadienyl radical (see Table 1). For the subsequent reactions, two possibilities exist. The first is for methyl substituents, e.g. m-toluate in Table 1. These compounds can react via the SET to generate a phenyl radical cation, which can then lose a benzylic proton, allowing rearranging into a more stable benzyl radical. A similar process can occur with phenols where again a SET leads to a phenyl radical cation which loses the acidic alcohol proton and following electron rearrangement produces a more stable phenoxide radical. This can also occur with the hydroxylated RAF product, hydroquinone radical which can further react to produce benzoquinone.

4. Conclusions

The thermodynamic and kinetic results for the SET reaction between SO_4^- and ACs provide insight into the application of SO_4^- based AOTs and ISCO. In order to maximize the oxidizing efficiency of SO_4^-, it is helpful to gain knowledge of the electron donating/withdrawing character of the substituents on target contaminants before applying SO_4^- based treatment technologies. With the better oxidizing selectivity for the contaminants in environmental matrix, the SO_4^- based AOTs exhibit high removal performance for aromatic contaminants with strong electron donating groups. In addition, our quantum mechanics-based calculations showed that the SET pathway will be the main reaction mechanism for the transformation of contaminants. Specifically, for benzoate compounds, decarboxylation of the carboxylate group on ACs may take place following the SET reaction. For other aromatic compounds, a SET reaction may occur from the aromatic ring generating a phenyl radical cation, and the subsequent reactions depend on the electronic effect of the functional groups on the phenyl ring. Therefore, knowing the reactivity of SO_4^- with environmental contaminants with specific functional groups is an important requirement in

the application and optimization of SO_4^- based advanced oxidation processes.

Acknowledgments

Appendix A. Supplementary data

Supplementary data associated with this article can be found, in the online version, at http://dx.doi.org/10.1016/j.cej.2017.06.179.

References

[1] M.M. Huber, S. Canonica, G.-Y. Park, U. Von Gunten, Oxidation of pharmaceuticals during ozonation and advanced oxidation processes, Environ. Sci. Technol. 37 (2003) 1016–1024.

[2] R. Xiao, D. Diaz-Rivera, L.K. Weavers, Factors influencing pharmaceutical and personal care product degradation in aqueous solution using pulsed wave ultrasound, Ind. Eng. Chem. Res. 52 (2013) 2824–2831.

[3] D. Vogna, R. Marotta, A. Napolitano, R. Andreozzi, M. d'Ischia, Advanced oxidation of the pharmaceutical drug diclofenac with UV/H$_2$O$_2$ and ozone, Water Res. 38 (2004) 414–422.

[4] W. Paul, S.P. Mezyk, W.J. Cooper, M. Daisuke, Electron pulse radiolysis determination of hydroxyl radical rate constants with Suwannee River fulvic acid and other dissolved organic matter isolates, Environ. Sci. Technol. 41 (2007) 4640–4646.

[5] R. Xiao, Z. Wei, D. Chen, L.K. Weavers, Kinetics and mechanism of sonochemical degradation of pharmaceuticals in municipal wastewater, Environ. Sci. Technol. 48 (2014) 9675–9683.

[6] R.Y. Xiao, Z.Q. He, D. Diaz-Rivera, G.Y. Pee, L.K. Weavers, Sonochemical degradation of ciprofloxacin and ibuprofen in the presence of matrix organic compounds, Ultrason. Sonochem. 21 (2014) 428–435.

[7] B. Zhang, Y. Zhang, Y. Teng, M. Fan, Sulfate radical and its application in decontamination technologies, Crit. Rev. Env. Sci. Technol. 45 (2015) 1756–1800.

[8] R. Xiao, T. Ye, Z. Wei, S. Luo, Z. Yang, R. Spinney, Quantitative structure-activity relationship (QSAR) for the oxidation of trace organic contaminants by sulfate radical, Environ. Sci. Technol. 49 (2015) 13394–13402.

[9] R. Norman, P. Storey, P. West, Electron spin resonance studies. Part XXV. Reactions of the sulphate radical anion with organic compounds, J. Chem. Soc. B (1970) 1087–1095.

[10] P. Neta, V. Madhavan, H. Zemel, R.W. Fessenden, Rate constants and mechanism of reaction of sulfate radical anion with aromatic compounds, J. Am. Chem. Soc. 99 (1977) 163–164.

[11] P. Caregnato, P.M.D. Gara, G.N. Bosio, M.C. Gonzalez, N. Russo, M.d.C. Michelini, D.O. Martire, Theoretical and experimental investigation on the oxidation of gallic acid by sulfate radical anions, J. Chem. Phys. 112 (2008) 1188–1194.

[12] P. O'Neill, S. Steenken, D. Schulte-Frohlinde, Formation of radical cations of methoxylated benzenes by reaction with OH radicals, Ti^{2+}, Ag^{2+}, and SO$_4^{rad-}$ in aqueous solution. An optical and conductometric pulse radiolysis and in situ radiolysis electron spin resonance study, J. Phys. Chem. 79 (1975) 2773–2779.

[13] K. Sehested, H. Corfitzen, H. Christensen, E. Hart, Rates of reaction of O$^-$ ions, ^{rad}OH, and H with methylated benzenes in aqueous solution. Optical spectra of radicals, J. Phys. Chem. 79 (1975) 310–315.

[14] T.C. An, H. Yang, G.Y. Li, W.H. Song, W.J. Cooper, X.P. Nie, Kinetics and mechanism of advanced oxidation processes (AOPs) in degradation of ciprofloxacin in water, Appl. Catal. B: Environ. 94 (2010) 288–294.

[15] H. Zemel, R.W. Fessenden, The mechanism of reaction of sulfate radical anion with some derivatives of benzoic acid, J. Phys. Chem. 82 (1978) 2670–2676.

[16] G. Tripathi, Electron-transfer component in hydroxyl radical reactions observed by time resolved resonance Raman spectroscopy, J. Am. Chem. Soc. 120 (1998) 4161–4166.

[17] T.C. An, Y.P. Gao, G.Y. Li, P.V. Kamat, J. Peller, M.V. Joyce, Kinetics and mechanism of ^{rad}OH mediated degradation of dimethyl phthalate in aqueous solution: Experimental and theoretical studies, Environ. Sci. Technol. 48 (2013) 641–648.

[18] J. Madhavan, F. Grieser, M. Ashokkumar, Combined advanced oxidation processes for the synergistic degradation of ibuprofen in aqueous environments, J. Hazard. Mater. 178 (2010) 202–208.

[19] R. Xiao, M. Noerpel, H. Ling Luk, Z. Wei, R. Spinney, Thermodynamic and kinetic study of ibuprofen with hydroxyl radical: A density functional theory approach, Int. J. Quantum Chem. 114 (2014) 74–83.

[20] G. Merga, C. Aravindakumar, B. Rao, H. Mohan, J. Mittal, Pulse radiolysis study of the reactions of SO$_4^{rad-}$ with some substituted benzenes in aqueous solution, J. Chem. Soc., Faraday Trans. 90 (1994) 597–604.

[21] T.A. Halgren, Merck molecular force field. II. MMFF94 van der Waals and electrostatic parameters for intermolecular interactions, J. Comput. Chem. 17 (1996) 520–552.

[22] M.J. Frisch, G.W. Trucks, H.B. Schlegel, G. E. Scuseria, M.A. Robb, J.R. Cheeseman, G. Scalmani, V. Barone, B. Mennucci, G.A. Petersson, H. Nakatsuji, M.Caricato, X. Li, H.P. Hratchian, A.F. Izmaylov, J. Bloino, G. Zheng, J.L. Sonnenberg, M. Hada, M. Ehara, K. Toyota, R. Fukuda, J. Hasegawa, M. Ishida, T. Nakajima, Y. Honda, O. Kitao, H. Nakai, T. Vreven, J.A. Montgomery, Jr., J.E. Peralta, F. Ogliaro, M. Bearpark, J.J. Heyd, E. Brothers, K.N. Kudin, V.N. Staroverov, T. Keith, R. Kobayashi, J. Normand, K. Raghavachari, A. Rendell, J.C. Burant, S.S. Iyengar, J. Tomasi, M. Cossi, N. Rega, J.M. Millam, M. Klene, J.E. Knox, J.B. Cross, V. Bakken, C. Adamo, J. Jaramillo, R. Gomperts, R. E. Stratmann, O. Yazyev, A.J. Austin, R. Cammi, C. Pomelli, J.W. Ochterski, R.L. Martin, K. Morokuma, V.G. Zakrzewski, G.A. Voth, P. Salvador, J.J. Dannenberg, S. Dapprich, A.D. Daniels, O. Farkas, J.B. Foresman, J.V. Ortiz, J.C.a.D. J., Fox Gaussian 09, Revision C. 01, Gaussian, Inc., Wallingford, CT, USA, 2010.

[23] A.D. Becke, Density-functional thermochemistry. III. The role of exact exchange, J. Chem. Phys. 98 (1993) 5648–5652.

[24] Y. Zhao, D.G. Truhlar, The M06 suite of density functionals for main group thermochemistry, thermochemical kinetics, noncovalent interactions, excited states, and transition elements: Two new functionals and systematic testing of four M06-class functionals and 12 other functionals, Theor. Chem. Acc. 120 (2008) 215–241.

[25] A.V. Marenich, C.J. Cramer, D.G. Truhlar, Universal solvation model based on solute electron density and on a continuum model of the solvent defined by the bulk dielectric constant and atomic surface tensions, J. Chem. Phys. B 113 (2009) 6378–6396.

[26] A.V. Marenich, C.J. Cramer, D.G. Truhlar, Performance of SM6, SM8, and SMD on the SAMPL1 test set for the prediction of small-molecule solvation free energies, J. Chem. Phys. B 113 (2009) 4538–4543.

[27] A.J. Salter-Blanc, E.J. Bylaska, M.A. Lyon, S.C. Ness, P.G. Tratnyek, Structure-activity relationships for rates of aromatic amine oxidation by manganese dioxide, Environ. Sci. Technol. 50 (2016) 5094–5102.

[28] D. Minakata, W. Song, J. Crittenden, Reactivity of aqueous phase hydroxyl radical with halogenated carboxylate anions: Experimental and theoretical studies, Environ. Sci. Technol. 45 (2011) 6057–6065.

[29] A. Galano, J.R. Alvarez-Idaboy, Kinetics of radical-molecule reactions in aqueous solution: a benchmark study of the performance of density functional methods, J. Comput. Chem. 35 (2014) 2019–2026.

[30] A.V. Marenich, J. Ho, M.L. Coote, C.J. Cramer, D.G. Truhlar, Computational electrochemistry: prediction of liquid-phase reduction potentials, Phys. Chem. Chem. Phys. 16 (2014) 15068–15106.

[31] R. Xiao, I. Zammit, Z. Wei, W. Hu, M. MacLeod, R. Spinney, Kinetics and mechanism of the oxidation of cyclic methylsiloxanes by hydroxyl radical in the gas phase: An experimental and theoretical study, Environ. Sci. Technol. 49 (2015) 13322–13330.

[32] C. Iuga, A. Campero, A. Vivier-Bunge, Antioxidant vs. prooxidant action of phenothiazine in a biological environment in the presence of hydroxyl and hydroperoxyl radicals: A quantum chemistry study, RSC Adv. 5 (2015) 14678–14689.

[33] Z. Yang, S. Luo, Z. Wei, T. Ye, R. Spinney, D. Chen, R. Xiao, Rate constants of hydroxyl radical oxidation of polychlorinated biphenyls in the gas phase: A single-descriptor based QSAR and DFT study, Environ. Pollut. 211 (2016) 157–164.

[34] Y. Gao, Y. Ji, G. Li, T. An, Mechanism, kinetics and toxicity assessment of OH-initiated transformation of triclosan in aquatic environments, Water Res. 49 (2014) 360–370.

[35] A. Galano, I. Alvarez, J. Raúl, Kinetics of radical-molecule reactions in aqueous solution: A benchmark study of the performance of density functional methods, J. Comput. Chem. 35 (2014) 2019–2026.

[36] R.A. Marcus, Chemical and electrochemical electron-transfer theory, Annu. Rev. Phys. Chem. 15 (1964) 155–196.

[37] R.A. Marcus, Electron transfer reactions in chemistry. Theory and experiment, Rev. Mod. Phys. 65 (1993) 599–610.

[38] A.J. Salter-Blanc, E.J. Bylaska, H.J. Johnston, P.G. Tratnyek, Predicting reduction rates of energetic nitroaromatic compounds using calculated one-electron reduction potentials, Environ. Sci. Technol. 49 (2015) 3778–3786.

[39] L. Eberson, Electron Transfer Reactions in Organic Chemistry, Springer Science & Business Media, 2012.

[40] D. Wang, Y. Li, M. Yang, M. Han, Decomposition of polycyclic aromatic hydrocarbons in atmospheric aqueous droplets through sulfate anion radicals: An experimental and theoretical study, Sci. Total Environ. 393 (2008) 64–71.

[41] M. Maroncelli, J. MacInnis, G.R. Fleming, Polar solvent dynamics and electron-transfer reactions, Science 243 (1989) 1674–1681.

[42] M.J. Weaver, Dynamical solvent effects on activated electron-transfer reactions: principles, pitfalls, and progress, Chem. Rev. 92 (1992) 463–480.

[43] C.I. Bayly, P. Cieplak, W. Cornell, P.A. Kollman, A well-behaved electrostatic potential based method using charge restraints for deriving atomic charges: The RESP model, J. Phys. Chem. 97 (1993) 10269–10280.

[44] T. Nakano, T. Kaminuma, T. Sato, K. Fukuzawa, Y. Akiyama, M. Uebayasi, K. Kitaura, Fragment molecular orbital method: Use of approximate electrostatic potential, Chem. Phys. Lett. 351 (2002) 475–480.

[45] P.I. Nagy, Competing intramolecular vs. intermolecular hydrogen bonds in solution, Int. J. Mol. Sci. 15 (2014) 19562–19633.

[46] T. Olmez-Hanci, I. Arslan-Alaton, Comparison of sulfate and hydroxyl radical based advanced oxidation of phenol, Chem. Eng. J. 224 (2013) 10–16.

[47] J. Holcman, K. Sehested, Anisole radical cation reactions in aqueous solution, J. Phys. Chem. 80 (1976) 1642–1644.

[48] I. Hussain, Y. Zhang, S. Huang, Degradation of aniline with zero-valent iron as an activator of persulfate in aqueous solution, RSC Adv. 4 (2014) 3502–3511.

[49] C. Hansch, A. Leo, R. Taft, A survey of Hammett substituent constants and resonance and field parameters, Chem. Rev. 91 (1991) 165–195.

[50] K.E. Pinkston, D.L. Sedlak, Transformation of aromatic ether- and amine-containing pharmaceuticals during chlorine disinfection, Environ. Sci. Technol. 38 (2004) 4019–4025.

[51] Y. Lee, U. Von Gunten, Quantitative structure–activity relationships (QSARs) for the transformation of organic micropollutants during oxidative water treatment, Water Res. 46 (2012) 6177–6195.